BOLETIN DE LA SOCIEDAD ESPAÑOLA DE
Cerámica y Vidrio
www.elsevier.es/bsecv

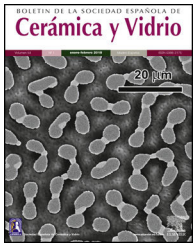

Mechanochemical and in vitro cytocompatibility evaluation of zirconia modified silver substituted 1393 bioactive glasses

Akher Ali[a,*], *Md Ershad*[a], *Sumit Hira*[b], *Ram Pyare*[a]

[a] *Department of Ceramic Engineering, Indian Institute of Technology (BHU), Varanasi 221005, Uttar Pradesh, India*
[b] *Department of Zoology, University of Burdwan, Purba Bardhaman 713104, West Bengal, India*

ARTICLE INFO

Article history:
Received 7 April 2020
Accepted 8 July 2020
Available online 6 August 2020

Keywords:
Glass ceramics
1393 bio-glass
Sol-gel
Cytocompatibility
Cell culture
Antibacterial activity

ABSTRACT

Zirconia and silver oxide substituted 1393 bioactive glasses (1393Zr and 1393Zr–1Ag) were prepared by sol-gel technique and sintered at 900–1100 °C. ZrO_2 incorporation into the glass was on the sole purpose of mechanical performance augmentation, while Ag_2O being antibacterial, their incorporation on microbial efficacy, in vitro bioactivity and cytocompatibility were assessed. The Ag_2O incorporated glass showed minimal effect on bioactivity of the parent glass. Both the cytocompatibility (U2-OS cells using MTT assay) and antibacterial efficacy (by using *Bacillus subtilis*; and *Escherichia coli*) were found significantly improved in silver doped glass than the undoped one. Excellent mechanical performance was also observed in 1393Zr-1Ag compared to the both pure 1393 glass and 1393Zr. Thus, Ag_2O incorporation into 1393Zr not only introduced the bactericidal efficacy, but also enhanced the mechanical properties of the glass, while leaving bioactivity unharmed. Thus the Ag_2O incorporated 1393Zr seems a potential biomaterial for bone tissue engineering application.

Evaluación de citocompatibilidad mecanoquímica e in vitro de vidrios bioactivos 1393 sustituidos con plata modificada con zirconia

Palabras clave:
Cerámica de vidrio
1393 bio-vidrio
Sol-gel
Citocompatibilidad
Cultivo celular
Actividad antibacterial

RESUMEN

Se prepararon vidrios bioactivos 1393 sustituidos con óxido de plata y circonia (1393Zr y 1393Zr-1Ag) mediante la técnica sol-gel y se sinterizaron a 900-1100 °C. La incorporación de ZrO2 en el vidrio tenía el único propósito de aumentar el rendimiento mecánico, mientras que Ag2O era antibacteriano, se evaluó su incorporación en la eficacia microbiana, la bioactividad in vitro y la citocompatibilidad. El vidrio incorporado Ag2O mostró un efecto mínimo sobre la bioactividad del vidrio original. Tanto la citocompatibilidad (células U2-OS usando el ensayo MTT) como la eficacia antibacteriana (usando B. subtilis y E. coli) se encontraron significativamente mejoradas en el vidrio dopado con plata que en el no dopado. También se observó un excelente rendimiento mecánico en 1393Zr-1Ag en comparación con

* *Corresponding author.*
E-mail address: akhera.rs.cer15@itbhu.ac.in (A. Ali).
https://doi.org/10.1016/j.bsecv.2020.07.002

el vidrio 1393 puro y el 1393Zr. Por lo tanto, la incorporación de Ag2O en 1393Zr no solo introdujo la eficacia bactericida, sino que también mejoró las propiedades mecánicas del vidrio, dejando intacta la bioactividad. Por lo tanto, el Ag2O incorporado 1393Zr parece un biomaterial potencial para la aplicación de ingeniería de tejido óseo.

Introduction

Bioactive glasses as described by Hench L.L. are a class of biomaterials, generally amorphous silicate based compounds, composed mainly of SiO_2, CaO, P_2O_5, and Na_2O [1]. The Bioactive glasses are able to bond to soft and hard tissues of bones by a series of reactions that produces a strong, compliant interface between the implant material and the host tissues [1,2]. Although, biomaterials can be prepared through several techniques, the most versatile one is sol gel method [1,3]. Here in our current investigation we preferred sol gel as a fabrication technique for synthesis of 1393 glass and their derivative. The low processing temperature, combined with the intrinsic biocompatibility (ability of not to produce a significant immunological rejection when they are inserted into the body) and environmental friendliness makes it an ideal technology for the fabrication of biomaterials [4–6]. Further, the process allows doping of various inorganic, organic and biomolecules during the formation of a glassy matrix [7–9].

However, the material under investigation in our present work is a zirconia modified Ag_2O substituted 1393 glass system. 1393 is a compositionally modified version of 45S5. A typical 1393 glass shall have SiO_2 – 53%, CaO – 20%, Na_2O – 6%, P_2O_5 – 4%, K_2O – 12% and MgO – 5% (wt%) [2,10]. 1393 has a facile viscous flow behavior, less devitrification tendency than that of 45S5 while the later is prone to crystallization during sintering.

Inorganic therapeutic ions/oxides often incorporate in biomaterials for improvement of physico-mechanical properties or biological responses at the implant–tissue interface [2,10–12]. The modification and substitution in 1393 glass with ZrO_2 and Ag_2O was aiming at different purposes. Zirconia addition in the glass system was to augent the flexural, compressive and elastic modulus of glass. Research suggests that the zirconia has a flexural strength of $>10^5$ times of atm (.1 MPa) [13] and compressive strength of ∼680 MPa [14] probably the highest among ceramic materials, which is why it is considered as 'ceramic steel'. Introduction Ag_2O was however on the sole purpose of cellular cytocompatibility, in vitro bioactivity study and bactericidal ability despite the fact that silver has many fascinating properties like the ability to confer microbial resiliency on biomedical materials and devices [15–20] and angiogenic inhibitor [21].

ZrO_2 as being nearly bio-inert in nature, when implanted shows only morphological fixation to the surrounding tissues without any chemical or biological bonding [1,22,23], it has been chosen to evaluate mechanical properties enhancement. However, preparation of zirconia NPs from their alkoxides is not very simplistic. Zirconium alkoxides are very moisture sensitive and they hydrolyze and condense so fast that the actual reaction rates are yet be determined. Here, we have prepared 1393 glasses with starting material zirconia by a stepwise hydrolysis of zirconium alkoxides and polymerization of hydrolyzed zirconium alkoxide [24–28]. Acetic acid was used as chelating agent to slow down the rate of hydrolysis. A Zr–O–Zr network was expected to obtain through hydrolysis and condensation

$$Zr(OC_4H_9)_4 + H_2O \rightarrow (OC_4H_9)_3Zr(OC_4H_9) + C_4H_9OH$$

$$(OC_4H_9)_3Zr(OH) + (OC_4H_9)_3Zr(OH) \rightarrow (OC_4H_9)_3Zr{-}O{-}Zr(OC_4H_9)_3 + C_4H_9OH$$

Materials and methods

Preparation of samples

Chemical compositions for preparation of the glasses are tabulated below (Table 1). 1393, zirconia modified 1393 (1393Zr) and Ag_2O substituted glass (1393Zr–1Ag) systems were prepared by sol-gel route using the precursors $SiC_8H_{20}O_4$ (Assay 98%, Sigma–Aldrich, US), $Ca(NO)_3{\cdot}4H_2O$, $Mg(NO)_3$, $NaNO_3$, KNO_3 (Assay > 99%, Loba chemie, IN), $C_6H_{15}O_4P$ (Assay 99%, Sigma–Aldrich, US), $Zr(OC_4H_9)_4$ (Assay 80% in 1-butanol, Sigma–Aldrich, US) and $AgNO_3$ (Assay 99%, Loba chemie, IN) respectively.

Starting from the preparation of zirconia by hydrolysis and condensation of zirconium butoxide as precursor followed by stepwise addition and complete hydrolysis of TEOS (Tetraethoxysilane), TEP (Triethylphosphate), calcium nitrate tetrahydrate, magnesium nitrate, potassium nitrate, sodium nitrate, and silver nitrate respectively in a magnetic stirrer at 50 °C maintaining the rpm 600 (Tarson digital spinot, IN). The mixing was continued for 1 h for each step to let complete the hydrolysis. The silver substituted glass specimen was stored in the dark place to preserve the +1 oxidation state of the silver ion. The prepared solutions were kept in a sealed Teflon container for 2 days at ambient temperature conditions for aging and gelation. The gel was then placed in a sealed container and heated at 80 °C for an additional 2 days period. To remove moisture and volatiles small holes were created on the lid to allow the leakage of gases and heat treated at 120 °C for 1 day to remove all the free water. The dried gel was then calcined for 24 h at 550 °C to eliminate residual nitrates and stabilize the glass.

The calcined glasses were ground with mortar and pestle and sieved. The powder samples were pelletized

Table 1 – Chemical composition (mol%).

Glasses	SiO_2	CaO	Na_2O	MgO	K_2O	ZrO_2	P_2O_5	Ag_2O
1393	54.66	22	6	7.7	7.9	0	1.74	0
1393Zr	52.66	22	6	7.7	7.9	2	1.74	0
1393Zr–1Ag	51.66	22	6	7.7	7.9	2	1.74	1

into 25 mm × 10 mm × 10 mm (rectangular) and 10 mm (height) × 10 mm (dia) (cylindrical) for flexural and compression property assessment respectively.

Preparation of SBF solution

The SBF solution was prepared according to the procedure described by Kokubo et al. [29], by dissolving NaCl 8.035 g/L, KCl 0.225 g/L, $K_2HPO_4{\cdot}3H_2O$ 0.231 g/L, $MgCl_2{\cdot}6H_2O$ 0.311 g/L, $CaCl_2$ 0.292 g/L, $NaHCO_3$ 0.355 g/L, and Na_2SO_3 0.072 g/L into distilled water, buffered at pH = 7.40 with 6.118 g/L tris-hydroxymethyl aminomethane and 1 N HCl solution at 37 °C. The SBF solution was chosen because of its characteristic of being highly supersaturated characteristic with respect to apatite. The SBF composition compared with human blood plasma where is shown in Table 2. According to Oyane and Takadama [30,31], the SBF solution is so far the best solution for in vitro measurement of apatite forming ability in implant materials. The pH of the SBF solution was measured using a digital pH meter after immersing the samples for different time periods.

In vitro bioactivity evaluation

0.25 g of each sample (powder) was soaked in 25 ml (10 mg/ml) of SBF solution and incubated at 37 ± 2 °C in a bacteriological incubator (Ikon, India) for 1,3,5,7 and 9 days. The powder were filtered, rinsed with double distilled water and dried in an oven (Ikon, India) at 100 °C for 4 h. To ensure the HA like layer formation the powdered samples were analyzed with pH, FTIR, XRD. Surface morphology of the solid samples was evaluated using SEM after 7 days of immersion.

pH

Behavioral changes in pH are evaluated after immersing the finely ground samples to SBF (10 mg/ml) for 1, 3, 5, 7, 9 days. pH values of the SBF solution was recorded using a digital pH meter (Universal Bio microprocessor, India) and for the corresponding days.

XRD

Powdered samples were analyzed using X-ray Diffractometer (RIGAKU-Miniflex II diffractometer adopted Cu-K_α radiation (λ = 1.5405 Å) with a tube current of 35 mA and voltage of 40 kV at 2θ = 10–80° with scanning rate 0.02°/s. The ICDS JCPDS Cards were used to analyze the peaks.

FTIR

Functional groups of glass samples were analyzed by subjecting powdered samples to a FTIR spectrometer (BRUKER Tensor, 27 FTIR, Germany) using the attenuated total reflection (ATR) method in the wavenumber range of 400–4000 cm^{-1}.

SEM

Modifications in surface morphology of the glass samples was performed using SEM (Inspect S50, FEI (US)) after soaking in SBF for 7 days. Glass surfaces were plasma coated by sputtering before SEM analysis.

Mechanical properties

The 3 point bend and compressive tests of rectangular (25 mm × 10 mm × 10 mm) and cylindrical (10 mm × 10 mm (Height × Diameter)) glass samples were analyzed using Universal Testing Machine (H10KL, Tinius Olsen, USA) at 0.5 mm/min crosshead speed, using a 10 KN load cell. Flexural strength, according to ASTM C1674-11 has been calculated by the equation

$$\sigma = \frac{3Pl}{2bd^2}$$

where P = applied load (N); l = outer span length of the specimen (mm); b = specimen width (mm); d = thickness of the sample (mm).

The modulus of elasticity (Young's modulus, shear modulus and bulk modulus) of the polished 1393, 1393Zr and 1393Zr-1Ag were measured using Olympus 45MG (USA) ultrasonic measurement gauge according to their standard directions. The ultrasonic sound wave velocity V_L (Longitudinal velocity) and V_T (Transverse velocity) that propagate through polished samples were measured using pulse echo technique in determination of those mechanical properties. The V12 broadband longitudinal wave transducer (10 MHz) and a V156 normal incidence transverse wave transducer (5 MHz) were used to perform the test as done elsewhere [12]. The Young's modulus (E), shear modulus (S) and bulk modulus (K) were calculated as per their (Olympus 45MG, USA) given equations

Young's Modulus $(E) = \frac{V_L^2\rho(1+\sigma)(1-2\sigma)}{1-\sigma}$

Shear Modulus $(S) = V_T^2\rho$

Bulk Modulus $(K) = \frac{E}{3(1-2\sigma)}$ where ρ is the density and σ is the Poisson's ratio the samples.

Chemical durability (By weight loss method)

Chemical durability is the resistance a glass offered toward an acidic or basic attack. Weight loss technique was used to measure the chemical durability of a glass [2,32]. Weight loss of the glass was calculated as

$$\%\,\text{Weight loss} = \frac{W_i - W_f}{W_i} \times 100$$

Table 2 – Concentrations of ion in human blood plasma and simulated body fluid.

Ions	Na^+	K^+	Mg^{2+}	Ca^{2+}	Cl^-	HCO_3^-	HPO_4^-	SO_4^-
Human blood plasma (mmol/L)	142	5	1.5	2.5	103.0	27	1.0	.5
SBF (mmol/L)	142.0	5.0	1.5	2.5	147.8	4.2	1.0	.5

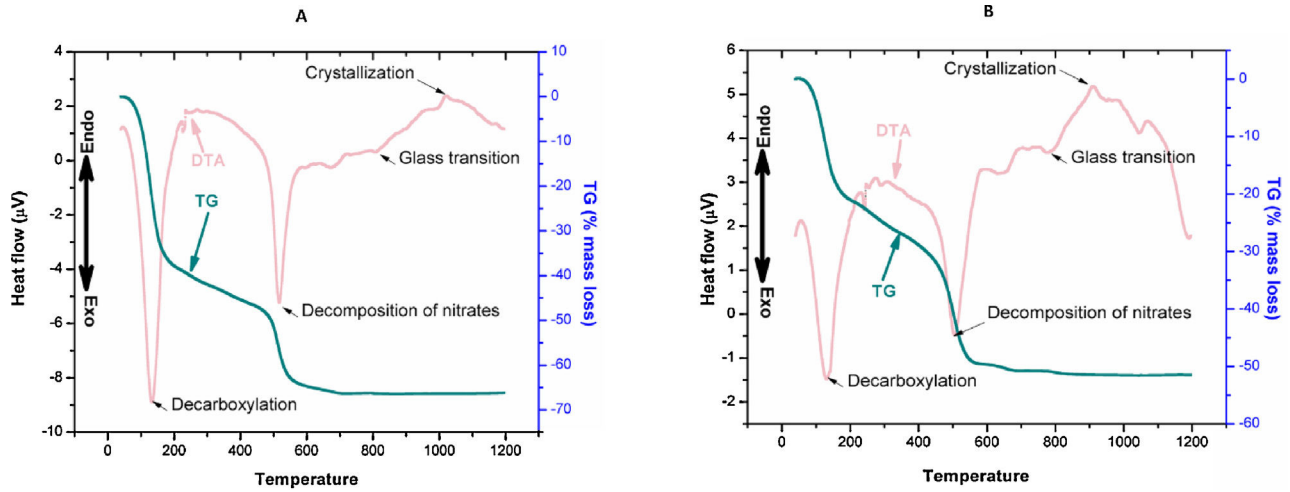

Fig. 1 – Differential thermal analysis (DTA) and thermo gravimetric (TG) analysis of (A) 1393Zr and (B) 1393Zr–1Ag.

Physiological assay

Cell culture

Human osteosarcoma cell (U2-OS) from American Type Culture Collection (ATCC, Manassas, USA) cultured in RPMI 1640 (Invitrogen, Carlsbad, CA) and supplemented with 10% fetal bovine serum (Hyclone, Logan, UT), 100 U/ml penicillin and 100 μg/ml streptomycin (Invitrogen, Carlsbad, CA), considered as complete medium. The cell line used here was free from mycoplasma. The PBMC (Peripheral blood mononuclear cell) cells were isolated from the freshly collected blood by Ficoll-Hypaque density gradient centrifugation technique and were washed with complete medium prior using for the assay

In vitro cell viability assay

In vitro cellular viability of U2-OS tumor cell was assessed after seeding upon 1393Zr and 1393Zr-1Ag using Colorimetric XTT (sodium 3-[1-(phenylaminocarbonyl)-3,4-tetrazolium]-bis(4-methoxy-6-nitro) benzene sulfonic acid hydrate) assay; (Roche Molecular Biochemicals, India). In a 96 well plate containing 5×10^3 cells/well were incubated for 48 h in a humidified (5% CO_2, @37 °C) atmosphere. Cell viability was calculated by measuring Optical density at 450 nm using Synergy HT Multi Mode Micro plate Reader (BioTek, USA) with the formula.

$$\%\,\text{Cell viability} = \frac{\text{Experimental OD}_{450}}{\text{Control OD}_{450}} \times 100$$

In vitro cell proliferation

Proliferative potential of 1393Zr and 1393Zr-1Ag was studied against the osteosarcoma cells (U2-OS) by MTT assay (Promega, USA) in a 96 wells tissue culture plate each containing 5×10^3 cells. After incubation for 48 h at different material concentrations (Concentration dependant) and at a material conc. of 2.5 mg/ml for varying time periods (Time dependant) in a 5% CO_2 humidified incubator @37 °C, the cells were exposed to the materials for cell growth inhibitory study. The % proliferation is calculated by the formula

$$\%\text{Growthinhibition} = \left[1 - \frac{\text{ExperimentalOD}_{570}}{\text{ControlOD}_{570}}\right] \times 100$$

where OD_{570} is the optical density or absorbance at wavelength 570 nm.

Cytoxicity

The lysis of bioactive samples was measured against U2-OS by cytotoxicity assay kit CytoTox 96® (Promega, USA). Materials were exposed to a 96 well tissue culture plate having 5×10^3 cells/well and incubated for 18 h at 37 °C in a humidified atmosphere. Lysis was determined using the formula.

$$\%\,\text{Cytotoxicity} = \frac{\text{Experimental} - \text{Effector Spontaneous} - \text{Target Spontaneous}}{\text{Target Maximum} - \text{Target Spontaneous}} \times 100$$

Antibacterial test

The antimicrobial efficacy of the 1393 bioactive glasses was performed against Gram positive *Bacillus subtilis* (MTCC 121) and Gram negative *Escherichia coli* (NCIM 5051). This study was done by bore-well method. Sterilized stainless steel borer of 9 mm diameter was used to make the bores into the agar plates. The glasses were taken in equal amount to put into the bores in different locations of the agar plates. To allow

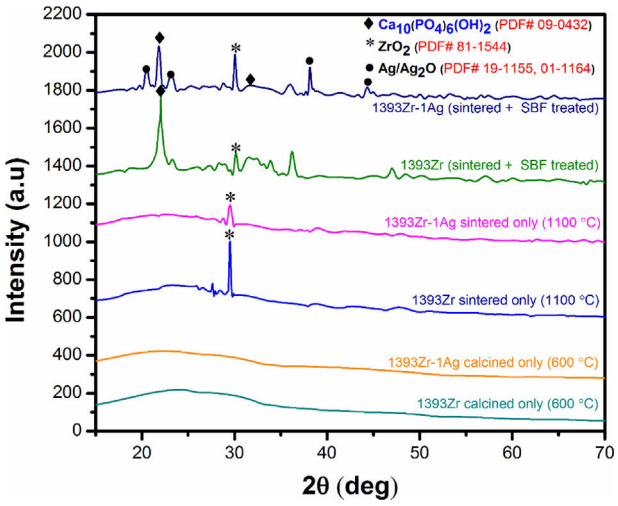

Fig. 2 – X-ray diffraction pattern of 1393Zr and 1393Zr-1Ag for calcined only (below two), sintered (1100 °C) (middle) and (B) soaked in SBF for 7 days (top two curves).

the growth of the bacteria the petri dishes were incubated at 37 ± 0.5 °C for 24 h. The inhibition zone was measured using a ruler after 24 h of incubation.

Statistical analysis

One way ANOVA followed by Tukey's test of mean comparison was performed using Prism6 graphpad while comparing between pairs. Each experiment was performed in triplicate and the data were presented as mean ± SD. Differences were considered significant for '*p*' value less than 0.05 (*), 0.01 (**) and 0.001 (***).

Results

Differential thermal analysis and thermo gravimetric analysis reveals many an information regarding the dehydration, decarboxylation, and glass transition and crystallization temperature. The first exothermic peaks (DTA) at 120–150 °C was for the mass loss (TG) due to removal of physically bonded water and residual volatiles. The second exothermic peak of mass loss was due to removal of nitrates. The third peak of DTA at 700–800 °C was the glass transition range. Onset nucleation and crystallization of the glasses due to controlled heat treatment were observed within 1000–1100 °C. However onset nucleation and crystallization temperatures were both reduced by almost 100 °C after Ag_2O incorporation to 1393Zr.

Fig. 2 corresponds to the XRD pattern of calcined (below), sintered (1100 °C) (middle) and soaked in SBF for 7 days (above) respectively. The figure illustrates the change in intensities of the corresponding samples soaked for a specified time period. For sintered only samples, there was a sharp peak at 2θ ~30° and a bump at 2θ ~20–30°. The major peaks became explicit for the soaked in SBF sample were at 2θ ~32°, 20–24° and 38–45°.

Fourier transform infrared spectroscopic analysis of the soaked in SBF glass samples (Fig. 3) shows the various vibrational peaks for different wavenumbers. The vibrational peaks at 460 cm^{-1}, 570 cm^{-1}, 796 cm^{-1}, 1040 cm^{-1}, 1370–1780 cm^{-1} and 2350–3800 cm^{-1} corresponds to several functional groups. The results illustrate that the vibrational peaks at 560 cm^{-1} and 796 cm^{-1} were exclusively explicit for SBF treated samples only.

Fig. 4A indicates the changes in pH of the glass samples soaked in SBF for 9 days. There was sharp increase in pH up to day 3 and a subsequent decrease after that. The decreasing rate of pH was reduced drastically and become almost constant after 7 days. The maximum pH value observed was 8.2 for silver incorporated samples at day 3. The chemical durability of the glasses against NaOH, HCl and SBF was represented

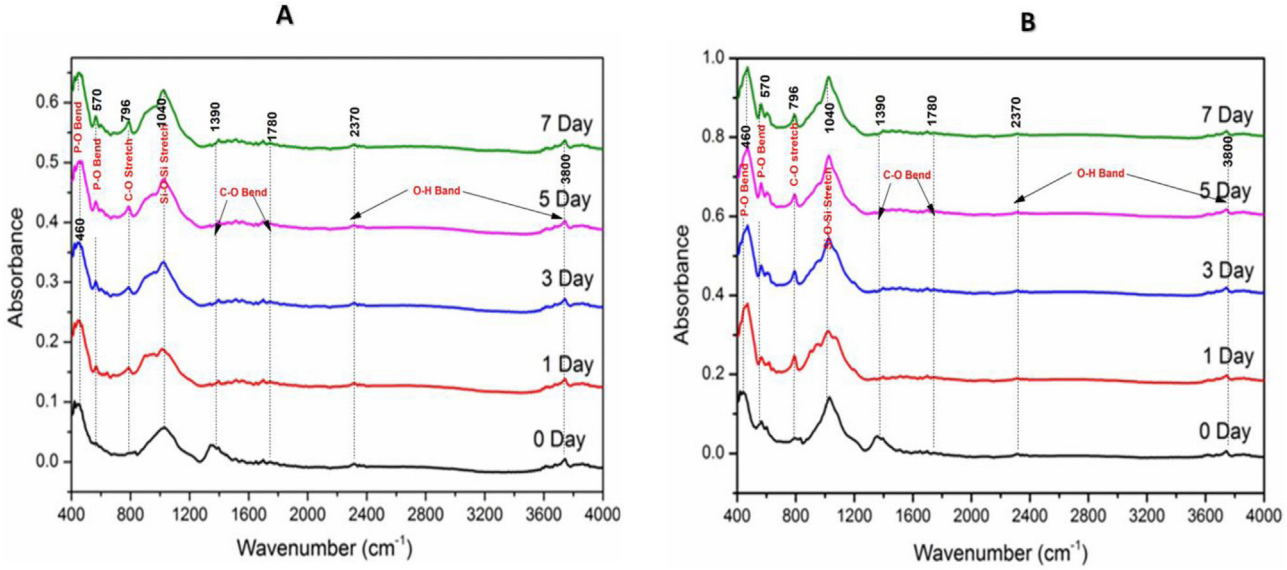

Fig. 3 – Fourier transform infrared spectral analysis for (A) 1393Zr and (B) 1393Zr–1Ag @ 4000–400 cm^{-1} wavenumber.

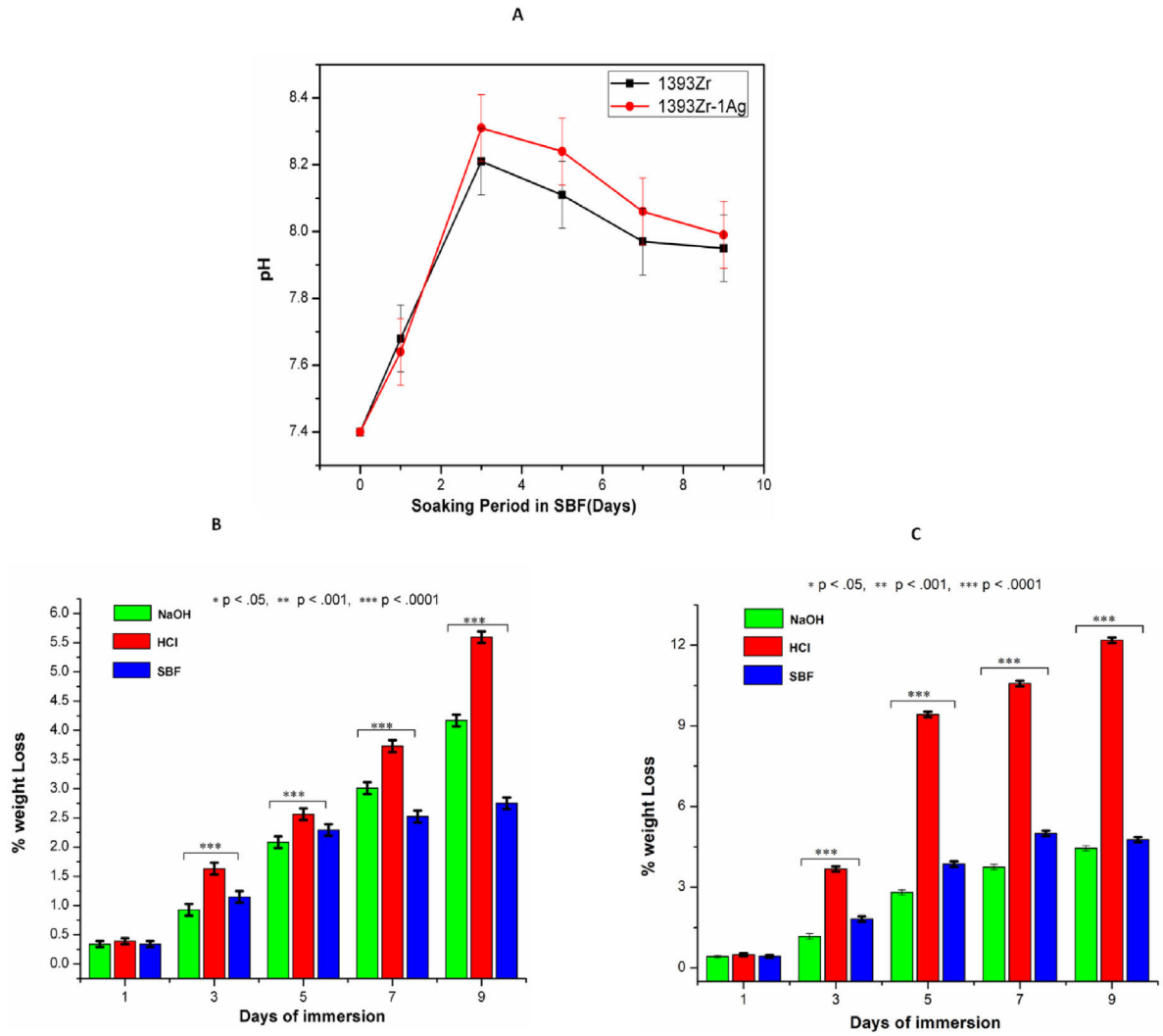

Fig. 4 – (A) pH and (B) Chemical Durability of 1393Zr and 1393Zr–1Ag as a function of material incubation time (days). One way Anova followed by Tukey's post hoc column wise mean comparison shows differences as not significant (ns), significant ($p < .05$) and highly significant ($p < .01$ and $p < .001$).

by Fig. 4B. The Percent weight loss of the glasses due to chemical attack by the aqueous solution was found maximum for silver doped one in HCl medium. Further, the weight loss % was found least for the glass samples kept in SBF solution.

Morphological analysis was depicted in Fig. 5 where 5A and Fig. 5B corresponds to the surface morphology of the pre SBF treated samples whereas 5C and 5D correspond to post SBF treated samples. Formation of cluster or spherical particles throughout the surface was found grown in the SBF treated samples.

Fig. 6(A → D) represents the mechanical and physical properties of the glasses. Our sol gel prepared 1393 glass sample was taken standard for mechanical performance evaluation after zirconia addition. The average (Mean ± SD; $n = 3$) compressive and flexural strengths of 1933, 1393Zr and 1393Zr-1Ag were 69, 98.43 and 110.33 MPa and 32.32, 41.23 and 44.67 MPa respectively. The Young's, Bulk and Shear modulus for the corresponding glasses were observed as 86.0, 82.3, 69.7 GPa; 89.1, 87.4, 78.0 GPa and 96.8, 92.4, 81.0 GPa respectively. Density of the glasses measured by Archimedes's principle was 2.68, 2.86 and 2.90 g/cc respectively.

Fig. 7A and B indicates the concentration dependant and time dependant inhibition of the cell growth kinetic study for the corresponding glasses. U2-OS cell line after being incubated in complete medium exposed the glass sample for proliferative study. The results illustrate that cell growth or their inhibition was insignificantly similar for both the glasses at same concentration. Similar results were observed for the time dependant kinetic study at a particular time period. Significant difference in cell growth inhibition was observed at a different material concentration or incubation time. Maximum cell growth (76.409%; Mean ± SD; $n = 3$) was found for 1393Zr @ 0.5 mg/ml material concentration where as in time dependant study the least inhibition (77.073%; Mean ± SD; $n = 3$) was found for 1393Zr-1Ag @ 24 h of incubation. Fig. 7C and D illustrates the Viability and Cytotoxicity for the corresponding glasses. The in vitro viability study reveals that the maximum viable cells of 95.655% was observed @ 0.5 mg/ml

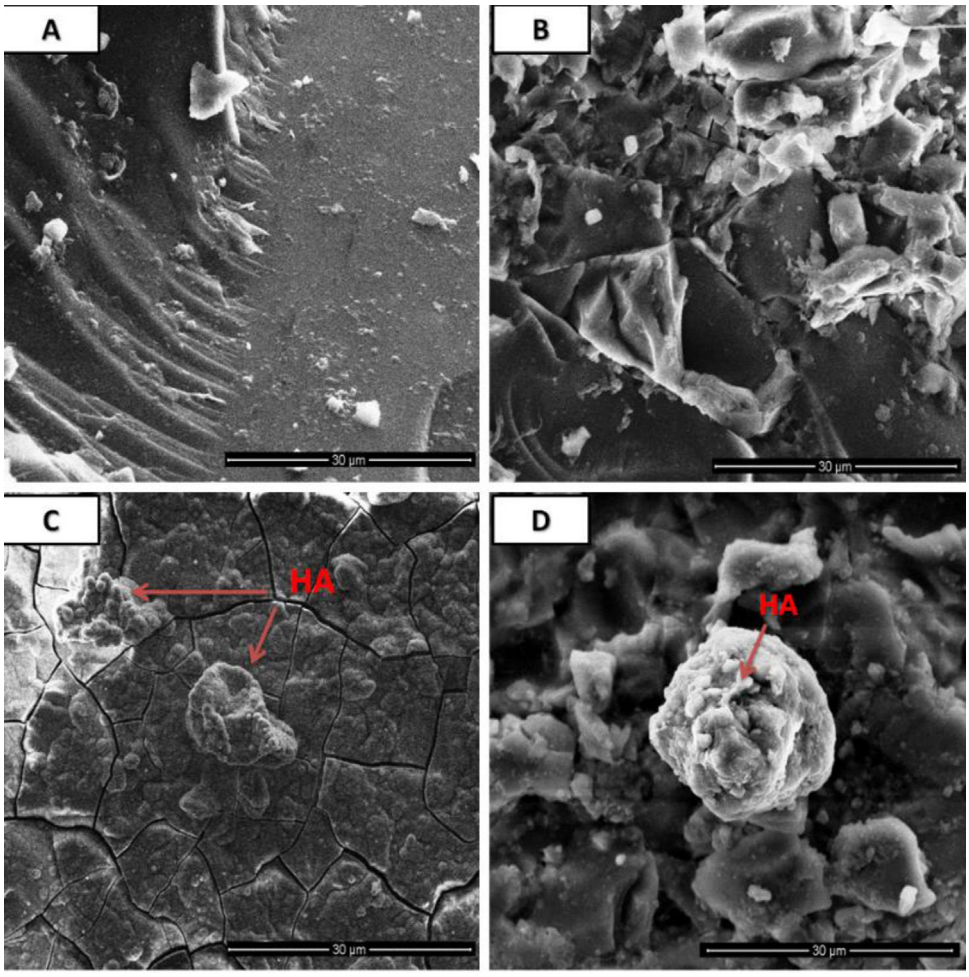

Fig. 5 – Surface morphological analysis by SEM of pre [(A) 1393Zr, (B) 1393Zr–1Ag] and post [(C) 1393Zr, (D) 1393Zr–1Ag] SBF treated samples.

concentration. Higher concentration of material found to lessen the viability. The 0.5 mg/ml concentration of materials was found to be least toxic as illustrated by Fig. 7D, where the % cytotoxicity observed was 11.009%.

Antimicrobial study (Fig. 8) for the corresponding bioactive glasses demonstrates that there was enhancement in bactericidal efficacy for the Ag_2O incorporated glasses for both Gram positive (*B. subtilis*) and Gram negative (*E. coli*) bacteria. The zone of inhibition for 1393Zr with the *B. subtilis* and *E. coli* environment was 4–4.3 mm whereas the inhibition zone was increased to 14–16 mm when the bacteria were grown in silver doped glass environment

Discussions

In our current investigation, we have observed from the DTA/TG curves (Fig. 1A and B) that the nucleation and crystallization temperature was reduced by the addition of network modifiers ions (Ag^+) to the glass system. The reduction in onset nucleation and crystallization temperature from 1020 °C for 1393Zr to 920 °C for 1393Zr–1Ag can be stated as the incorporation of Ag_2O might have acted as network modifier to decrease the bridging oxygens of glasses, thus resulting in lowering bond strength. Further, Ag_2O was believed to have acted as a nucleating agent for the glass system which is why nucleation and crystallization temperature have reduced [33]. However, this nucleation and crystallization temperature was an important parameter in determining the sintering temperature of glasses.

Bioactivity of any bioactive materials is validated by the evolution of hydroxy-carbonated apatite (HCA) layer under physiological conditions [2,40]. XRD analysis was proven to be a useful methodology in determination of the HA like layer. In our current experiment, we have measured the X-Ray diffraction peaks to confirm the presence of HA like layer. Our observed results for the soaked in SBF samples (Fig. 2, top two curves) indicate that the intense peak at $2\theta = 32°$, 22° and 38° can be attributed due to the presence of crystalline hydroxypatite (PDF # 09-0432) [2,34] which is also supported by our pH, SEM and FTIR analysis. The other peaks at $2\theta = 20°$, 23° and 45° corresponds to crystalline Ag/Ag_2O (PDF # 19-1155, 01-1164, 42-0874) while the sharp peak at $2\theta = 30°$ can be assigned to the crystalline ZrO_2 (PDF # 81–1544). The less intense wide hump between $2\theta = 20–30°$ was due to the destructive interference leading to a bump instead of sharp peaks, corresponds

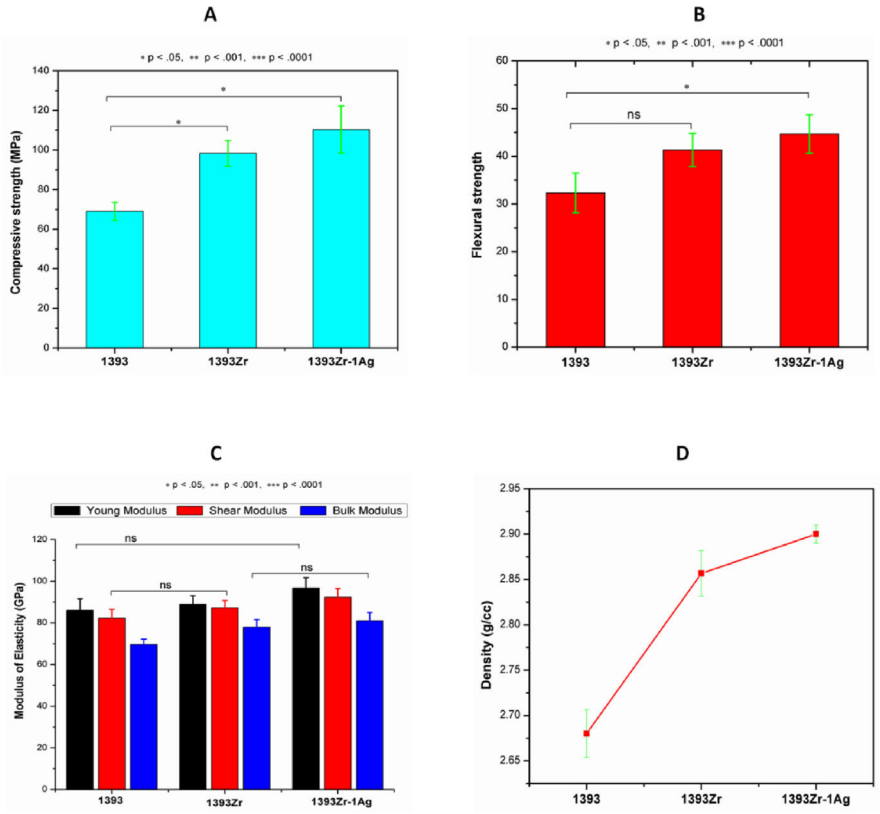

Fig. 6 – Physical and mechanical properties of the glass samples as (A) Compression, (B) flexure, (C) Modulus of elasticity and (D) Density. One way Anova followed by Tukey's post hoc column wise mean comparison test indicates differences in properties as not significant (ns), significant ($p < .05$) and highly significant ($p < .01$ and $p < .001$) ($n = 3$, Mean ± SD).

to the glassy nature of the samples. Thus the results illustrate that, the glasses are bioactive in nature and Ag_2O addition to the parent glass system did not affect their bioactive efficacy.

FTIR spectroscopic spectral analysis (Fig. 3A and B) corresponds to the functional groups for the individual molecules present in our glass compounds. The result demonstrates the trifling differences in the IR spectra between our two glass samples. The primary IR spectral vibrations for Si—O—Si functional units were comprised of bending mode at ~460 cm^{-1} and stretching at 800–1100 cm^{-1} [2,35]. The bending vibrational peaks at 460 cm^{-1} was attributed to the characteristic peak for the silicate glasses. It is believed that the P—O bond within the range of 500–800 cm^{-1} is the evidence for the formation of HCA layer [35], which implies the vibrational bonds for the SBF treated glasses at 570 cm^{-1} and 796 cm^{-1} was due to the bending vibration of P—O bond. The spectral vibrational bonds at 1040 cm^{-1} and 570 cm^{-1} become intense over soaking time, which was due to the plausible overlapping of the PO_4^- bond with the preexisting Si-O-Si bands. Thus, the evolution of P—O bands at various spectral value (wavenumber) was an indication of bioactive nature of our glasses.

The HA like layer formation is believed to be estimated by behavioral change of pH in simulated body fluid [2,11,12,36–38]. The rapid increase in pH for the first 3 days was due to the dissolution and fast ion exchange from the surface of the glasses with the SBF solution [11,12]. The results (Fig. 4A) illustrate that the quicker increase in pH for the Ag incorporated glass was due to the probable increase of non-bridging oxygens and subsequent decrease in bond strength after addition of network modifiers (Ag_2O). Ag_2O incorporation to the parent glass system could have also distorted and weakened the glass network because of their difference in ionic radius [Ag^{1+} = 115 pm, Si^{4+} = 40 pm) [2], which eventually led faster release of ions. However increase in basicity of the SBF solution due to ion release was previously shown enhancing HA like layer formation ability. Higher pH facilitates higher formation of silanols (—SiOH) through hydrolysis and their subsequent polymerization caused to form alkali ions (Na^+, Ca^{2+}) depleted silica rich layer [39–41]. The reduction in pH after 3 day was due to the continuous dissolution of the glass resulted in coupling the Ca^{2+} and PO_4^- ions from the solution to promote the HA like layer [42]. The HA layer formed due to coupling of those species (e.g. Ca^{2+} and PO_4^-) on the SiO_2 rich layer gradually cut the connectivity between the glass surface and SBF solution, thus the decrease in pH were observed after day 3.

Fig. 4B and C demonstrates that percent weight loss of bioactive glasses were higher for Ag_2O incorporated glass system. The results illustrate that the glasses immersed in HCl were observed with higher weight loss. The least weight loss of glasses was however observed in those that immersed in SBF. As the chemical durability is inversely proportional to the weight loss, the glasses with silver found to be least durable for all environments.

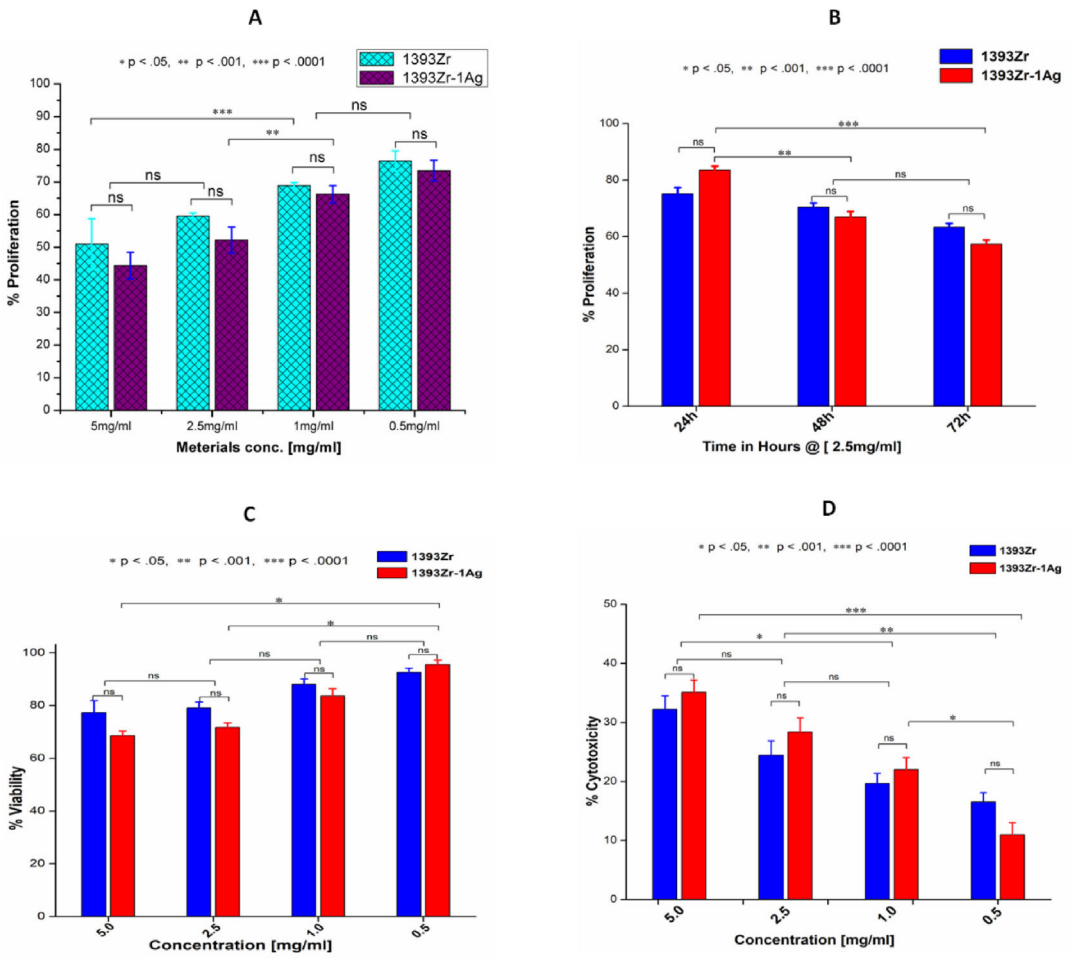

Fig. 7 – (A) Concentration dependant proliferation @ 48 h (B) Time dependant tumor cell proliferation @ 2.5 mg/ml (C) Tumor cell viability @ 18 h and (D) Cytoxicity @ 18 h of the 1393Zr and 1393Zr–1Ag glass samples against U2-OS cell line using MTT assay (Promega, USA), where 5 x 10^3 cells were plated in each of 96 well plates and cultured in complete medium with different concentrations/ time periods at 37 °C in 5% CO_2 humidified atmosphere. One way ANOVA using Tukey's post hoc test to perform column wise significant analysis for the *p* value < .05, < .01 and *p* < .001) indicates their changes after Ag incorporation to the parent glass system (*n* = 3, Mean ± SD).

The surface morphological micrograph of SBF treated samples (Fig. 5C and D) reveal the formation of irregular shaped HCA crystal in the form of agglomeration or dispersed particles throughout the glass surface. The carbonated layer have for both 1393Zr and 1393Zr–1Ag glass samples. The formation of HCA was also supported by XRD, pH and FTIR analysis.

To ensure the ZrO_2 addition to the glasses has augmented the mechanical properties, our sol gel derived 1393 glass was taken for the comparative property evaluation. One way ANOVA followed by Tukey's pair wise mean comparison was used to check significant ($p < 0.05$) differences in their properties. The results were taken in triplicate and their mean was compared. The result demonstrates that the compression and flexure strength (Fig. 6A and B) of the glasses have been improved significantly, while there were insignificant improvements in elastic moduli (Fig. 6C). Further there was enhancement in density after addition of zirconia and silver oxide to the glasses. These could be due to the replacement of lighter atoms (Si = 14) with the heavier ones (Zr = 40, Ag = 47). Further, partially substitution of the smaller ions (Si^{4+} = 40pm) with the larger ones (Zr^{4+} = 86, Ag^{1+} = 115 pm) could have resulted in compactness enhancement and their subsequent improvements in mechanical properties [43].

The cell growth, cell survival and cell lysis study were demonstrated by Fig. 7A–D. Statistical analysis demonstrates that there was no significant cell growth inhibition at same material concentration for concentration dependant proliferation. However, the growth was inhibited significantly for higher material concentrations. In time dependant proliferation (@2.5 mg/ml material conc.) significant decrease in cell growth was observed for the 72 h study. The 48 h cell viability study also suggests that the higher material concentration results in significant decrease in their endurance. Result illustrates the maximum cell survival at 0.5 mg/ml concentration. Highest percent of viable cells observed for 1393Zr–1Ag was 95.66% at 0.5 mg of material in 1 ml medium. The cell cytotoxicity study also suggest that the higher concentration of our glass samples proven to be toxic to the U2-OS tumor cells. The results also demonstrate that, Ag incorporation to the glasses has vaguely reduced the viability and proliferation and

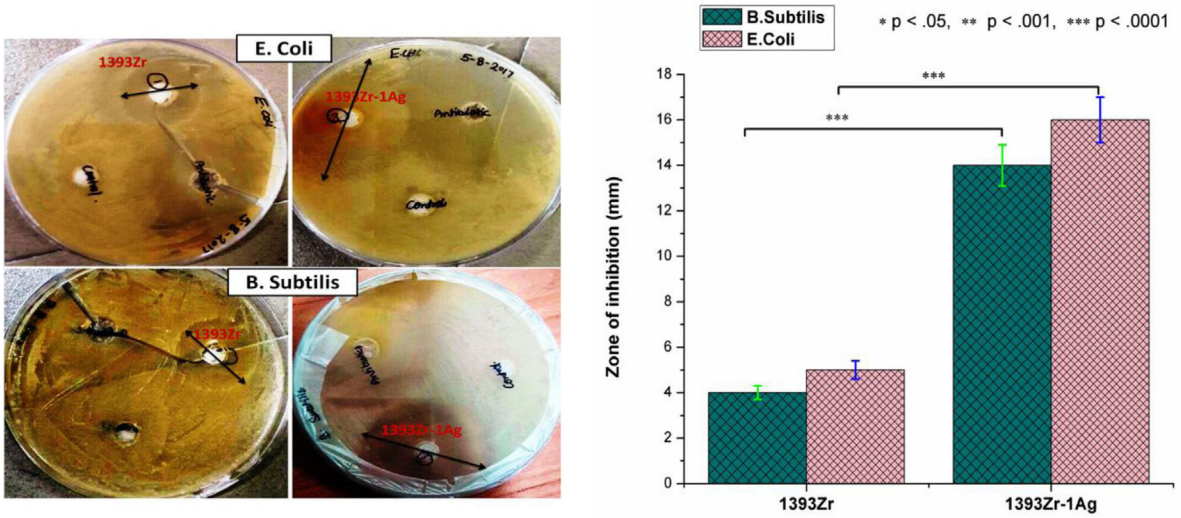

Fig. 8 – Bactericidal efficacy test of Ag_2O substituted bioactive 1393Zr glass. Statistical analysis shows significant gram positive (*B. subtilis*) and Gram negative (*E. coli*) bacterial growth inhibition after Ag_2O incorporation to the glass ($n = 3$, Mean ± SD).

increased cytotoxicity which could be due to their probable antibacterial and antiangiogenic nature [3]. From the cell culture and their cytocompatibility study it is evident that the glasses are cytotoxic, fatal and lytic to cells at higher concentration but at lower concentration (<0.5 mg/ml) they are found to be cytocompatible.

The bactericidal efficacy test for the corresponding bioactive glasses reveal that there was significant broadening of the zone of inhibition for the Ag_2O substituted glass. The enhancement in inhibition zone for the Ag_2O substituted glass could be due to the bactericidal ability of the Ag particles [44]. Further, due to the increased leachability of the ions after addition of network modifiers (Ag^+) as discussed earlier, the bacterial growth inhibition might have augmented momentously. Hence, the result confirmed that there was considerable enhancement in bactericidal efficiency after Ag_2O incorporation to the parent glass.

Conclusions

We have successfully prepared the zirconia modified Ag_2O substituted 1393 glasses by sol gel technique. Zirconia incorporation to the glasses aiming at mechanical properties augmentation was evaluated. cytocompatibility performance assessment was also evaluated after Ag_2O incorporation. The mechanical property evaluation study confirms their obvious improvement in compressive and flexural strength and trivial improvements in modulus of elasticity. In vitro study to assess bioactivity of these glasses substantiates the formation of HCA like layer. MTT assay demonstrate their moderate levels of cell lysis at high concentration of materials. The optimal viability and cell growth and minimal cytotoxicity was observed at lower concentration of materials. Further, the bactericidal efficacy test for Ag_2O substituted bioactive 1393Zr glass confirms significant improvement in antibacterial ability of glass. The chemical durability study also suggests their optimal compatibility with physiological fluid. Finally, although these glasses fit suitable by the in vitro study, their application in tissue engineering requires further in vivo validation.

Acknowledgements

The author (Akher Ali) gratefully acknowledges the Ministry of Human Resource Development, India (MHRD, India) and Indian Institute of technology (BHU), INDIA for providing financial support and Department of Ceramic Engineering, IIT (BHU) for providing necessary facilities to conduct the research work.

REFERENCES

[1] L.L. Hench, R.J. Splinter, W. Allen, T. Greenlee, Bonding mechanisms at the interface of ceramic prosthetic materials, J. Biomed. Mater. Res. 5 (6) (1971) 117–141.
[2] A. Ali, M. Ershad, V.K. Vyas, S.K. Hira, P.P. Manna, B. Singh, S. Yadav, P. Srivastava, S. Singh, R. Pyare, Studies on effect of CuO addition on mechanical properties and in vitro cytocompatibility in 1393 bioactive glass scaffold, Mater. Sci. Eng. C 93 (2018) 341–355.
[3] M. Bellantone, H.D. Williams, L.L. Hench, Broad-spectrum bactericidal activity of Ag_2O-doped bioactive glass, Antimicrob. Agents Chemother. 46 (6) (2002) 1940–1945.
[4] J. Bejarano, P. Caviedes, H. Palza, Sol–gel synthesis and in vitro bioactivity of copper and zinc-doped silicate bioactive glasses and glass-ceramics, Biomed. Mater. 10 (2) (2015) 025001.
[5] R. Li, A. Clark, L. Hench, An investigation of bioactive glass powders by sol-gel processing, J. Appl. Biomater. 2 (4) (1991) 231–239.
[6] P. Sepulveda, J.R. Jones, L.L. Hench, Characterization of melt-derived 45S5 and sol-gel-derived 58S bioactive glasses, J. Biomed. Mater. Res. 58 (6) (2001) 734–740.
[7] V. Mourino, J.P. Cattalini, A.R. Boccaccini, Metallic ions as therapeutic agents in tissue engineering scaffolds: an overview of their biological applications and strategies for new developments, J. R. Soc. Interface 9 (68) (2011) 401–419.
[8] A. Hoppe, N.S. Güldal, A.R. Boccaccini, A review of the biological response to ionic dissolution products from bioactive glasses and glass-ceramics, Biomaterials 32 (11) (2011) 2757–2774.
[9] A. Hoppe, V. Mouriño, A.R. Boccaccini, Therapeutic inorganic ions in bioactive glasses to enhance bone formation and beyond, Biomater. Sci. 1 (3) (2013) 254–256.
[10] A.M. Deliormanlı, Electrospun cerium and gallium-containing silicate based 13–93 bioactive glass fibers for biomedical applications, Ceram. Int. 42 (1) (2016) 897–906.
[11] V.K. Vyas, A.S. Kumar, A. Ali, S. Prasad, P. Srivastava, S.P. Mallick, M. Ershad, S.P. Singh, R. Pyare, Assessment of nickel oxide substituted bioactive glass-ceramic on in vitro bioactivity and mechanical properties, Boletín de la Sociedad Española de Cerámica y Vidrio 55 (6) (2016) 228–238.
[12] M. Ershad, V.K. Vyas, S. Prasad, A. Ali, R. Pyare, Effect of Sm_2O_3 substitution on mechanical and biological properties of 45S5 bioactive glass, J. Aust. Ceram. Soc. 54 (4) (2018) 621–630.
[13] J. Jones, A. Clare, Bio-glasses: An Introduction, John Wiley & Sons, 2012.
[14] U. Hambire, V. Tripathi, Optimization of compressive strength of zirconia based dental composites, Bull. Mater. Sci. 37 (6) (2014) 1315–1320.
[15] P. Newby, R. El-Gendy, J. Kirkham, X. Yang, I. Thompson, A. Boccaccini, Ag-doped 45S5 Bioglass®-based bone scaffolds by molten salt ion exchange: processing and characterisation, J. Mater. Sci.: Mater. Med. 22 (3) (2011) 557–569.
[16] A. Adams, E. Santschi, M. Mellencamp, Antibacterial properties of a silver chloride-coated nylon wound dressing, Vet. Surg. 28 (4) (1999) 219–225.
[17] N. Gatter, W. Kohnen, B. Jansen, In vitro efficacy of a hydrophilic central venous catheter loaded with silver to prevent microbial colonization, Zentralblatt für Bakteriologie 287 (1–2) (1998) 157–169.
[18] M. Kawashita, S. Tsuneyama, F. Miyaji, T. Kokubo, H. Kozuka, K. Yamamoto, Antibacterial silver-containing silica glass prepared by sol–gel method, Biomaterials 21 (4) (2000) 393–398.
[19] T. Kim, Q.L. Feng, J. Kim, J. Wu, H. Wang, G. Chen, F. Cui, Antimicrobial effects of metal ions (Ag^+, Cu^{2+}, Zn^{2+}) in hydroxyapatite, J. Mater. Sci.: Mater. Med. 9 (3) (1998) 129–134.
[20] T. Matsuura, Y. Abe, Y. Sato, K. Okamoto, M. Ueshige, Y. Akagawa, Prolonged antimicrobial effect of tissue conditioners containing silver-zeolite, J. Dent. 25 (5) (1997) 373–377.
[21] N. Hashemi Goradel, F. Ghiyami-Hour, S. Jahangiri, B. Negahdari, A. Sahebkar, A. Masoudifar, H. Mirzaei,

Nanoparticles as new tools for inhibition of cancer angiogenesis, J. Cell. Physiol. 233 (4) (2018) 2902–2910.
[22] A. Marti, Inert bioceramics (Al_2O_3, ZrO_2) for medical application, Injury 31 (2000) D33–D36.
[23] W. June, An introduction to bioceramics, World Sci. (1993).
[24] T. Ogihara, N. Mizutani, M. Kato, Growth mechanism of monodispersed ZrO_2 particles, J. Am. Ceram. Soc. 72 (3) (1989) 421–426.
[25] H. Kumazawa, Y. Hori, E. Sada, Synthesis of spherical zirconia fine particles by controlled hydrolysis of zirconium tetrabutoxide in 1-propanol, Chem. Eng. J. 51 (3) (1993) 129–133.
[26] T. Ogihara, N. Mizutani, M. Kato, Processing of monodispersed ZrO_2 powders, Ceram. Int. 13 (1) (1987) 35–40.
[27] E.W. Leib, U. Vainio, R.M. Pasquarelli, J. Kus, C. Czaschke, N. Walter, R. Janssen, M. Müller, A. Schreyer, H. Weller, Synthesis and thermal stability of zirconia and yttria-stabilized zirconia microspheres, J. Colloid Interface Sci. 448 (2015) 582–592.
[28] J. Widoniak, S. Eiden-Assmann, G. Maret, Synthesis and characterisation of monodisperse zirconia particles, Eur. J. Inorg. Chem. 2005 (15) (2005) 3149–3155.
[29] T. Kokubo, H. Kushitani, S. Sakka, T. Kitsugi, T. Yamamuro, Solutions able to reproduce in vivo surface-structure changes in bioactive glass-ceramic A-W3, J. Biomed. Mater. Res. 24 (6) (1990) 721–734.
[30] A. Oyane, K. Onuma, A. Ito, H.M. Kim, T. Kokubo, T. Nakamura, Formation and growth of clusters in conventional and new kinds of simulated body fluids, J. Biomed. Mater. Res. A 64 (2) (2003) 339–348.
[31] H. Takadama, M. Hashimoto, M. Mizuno, T. Kokubo, Round-robin test of SBF for in vitro measurement of apatite-forming ability of synthetic materials, Phosphor. Res. Bull. 17 (2004) 119–125.
[32] A. Paul, Chemical durability of glasses; a thermodynamic approach, J. Mater. Sci. 12 (11) (1977) 2246–2268.
[33] D. Bahadur, N. Sudhakar, S. Sharma, K. Gupta, A. Majumdar, Ag_2O as nucleating agent in the crystallization of superconducting phase in $Bi_2Sr_2Ca_4Cu_{5-y}$ glass composition, Phys. C: Superconduct. 190 (4) (1992) 527–536.
[34] N.H. Camargo, S.A. de Lima, E. Gemelli, Synthesis and characterization of hydroxyapatite/TiO_{2n} nanocomposites for bone tissue regeneration, Am. J. Biomed. Eng. 2 (2) (2012) 41–47.
[35] A.M. Deliormanlı, Preparation, in vitro mineralization and osteoblast cell response of electrospun 13–93 bioactive glass nanofibers, Mater. Sci. Eng. C 53 (2015) 262–271.
[36] S.K. Yadav, S. Ray, M. Ershad, V.K. Vyas, S. Prasad, A. Ali, S. Yadav, M.R. Majhi, R. Pyare, Development of zirconia substituted 1393 bioactive glass for orthopaedic application, 2017.
[37] S.K. Yadav, V.K. Vyas, S. Ray, M. Ershad, A. Ali, S. Prasad, M.R. Majhi, R. Pyare, In vitro Q2bioactivity and mechanical properties of zirconium dioxide doped 1393 bioactive glass, 2020.
[38] M. Ershad, V.K. Vyas, S. Prasad, A. Ali, R. Pyare, Synthesis and characterization of cerium-and lanthanum containing bioactive glass, Key Eng. Mater. Trans. Tech. Publ. (2017) 617–628.
[39] L.L. Hench, Bioceramics: from concept to clinic, J. Am. Ceram. Soc. 74 (7) (1991) 1487–1510.
[40] A. Ali, B.N. Singh, S.K. Hira, S. Singh, R. Pyare, ZnO modified 1393 bioactive scaffolds with enhanced cytocompatibility and mechanical performance, Ceram. Int. 46 (5) (2020) 6703–6713.
[41] M. Ershad, A. Ali, N.S. Mehta, R.K. Singh, S.K. Singh, R. Pyare, Mechanical and biological response of ($CeO_2 + La_2O_3$)-substituted 45S5 bioactive glasses for biomedical application, J. Aust. Ceram. Soc. (2020) 1–10.
[42] A. Goel, R.R. Rajagopal, J.M. Ferreira, Influence of strontium on structure, sintering and biodegradation behaviour of $CaO–MgO–SrO–SiO_2–P_2O_5–CaF_2$ glasses, Acta Biomater. 7 (11) (2011) 4071–4080.
[43] D. Bellucci, A. Sola, V. Cannillo, Bioactive glass/ZrO_2 composites for orthopaedic applications, Biomed. Mater. 9 (1) (2013) 015005.
[44] S. Gurunathan, K.-J. Lee, K. Kalishwaralal, S. Sheikpranbabu, R. Vaidyanathan, S.H. Eom, Antiangiogenic properties of silver nanoparticles, Biomaterials 30 (31) (2009) 6341–6350.